Trojan wave packets: Mathieu theory and generation from circular states

Maciej Kalinski and J. H. Eberly
Department of Physics and Astronomy, University of Rochester, Rochester, New York 14627
(Received 13 September 1995)

We present an analytic theory of three-dimensional Trojan (stable nonspreading) wave packets. The theory is valid beyond the harmonic approximation presented previously. We show that electron wave packets that are both radially and angularly well localized can be generated from an angularly completely delocalized state (a circular Rydberg state) by adiabatic switching of a circularly polarized electric field. Confinement of the Rydberg electron results from the suppression of the nonlinearity of the Coulomb spectrum, the same nonlinearity that is responsible for wave-packet spreading and revivals in the absence of the applied field. A comparison with the harmonic approach is also presented, as well as the results of numerical experiments based on integration of the time-dependent and field-dependent Schrödinger equation for the electron.

PACS number(s): 32.80.Rm, 42.50.Hz, 95.10.Ce

I. INTRODUCTION

We have shown [1–3] that the collective action of the Coulomb potential and a circularly polarized electric field leads to both the angular and the radial confinement of a hydrogenic electron moving in a circular near-Rydberg orbit. The origin of this phenomenon lies in the stability of a classical orbit [4], but the packet is much more stable than one could expect from its classical properties [5]. Because of a close analogy with asteroid stability in planetary mechanics, we call these probability distributions Trojan wave packets.

This stability enhancement can be understood from the hydrodynamic formulation of quantum mechanics [6]. Within the hydrodynamic approach the packet can be thought of as an ensemble of particles distributed according to the true quantum probability density moving in both classical and quantum potentials. The quantum potential depends on the probability density itself in a nonlocal way and can produce a drastic difference between the quantum and the classical behavior. By proper choice of the packet shape one can increase the stability of the classical potential [7] and even cause probability localization around trajectories that are classically unstable [8].

Our recent numerical results [3] show that Trojan packets exist even for low values of the angular momentum (on the order of 10). Similar electron confinement could be achieved using a magnetic field in the case of a free electron (Landau packets) when the cyclotronic frequency of the field is of the order of the frequency of the circularly polarized field. The existence of Trojan packets for low angular momenta (high frequencies) provides a dynamic situation equivalent to the focusing effect of magnetic fields on the order of 100 T, which cannot be reached yet in laboratory experiments.

Interest in the experimental study of Rydberg atoms in microwave and other fields is continuously growing [9–17]. Rydberg wave-packet formation is an important part of those studies [18–22] and we believe Trojan wave packets would be interesting to observe.

In the following we present a theory of Trojan wave packets that is valid outside the harmonic domain of our first study [1]. It works for lower values of the electric field when the wave packet is less confined and the harmonic approximation can break down. Section II demonstrates how the approximate energy spectrum and eigenfunctions can be obtained from the wave function expansion in hydrogenic basis through the theory of Mathieu functions. In Sec. III we show the connection between the basis expansion method and the harmonic approximation used originally in [1]. In Sec. IV we demonstrate which manifolds of hydrogenic states are related to the eigenstates of our harmonic Hamiltonian. The applicability of the model for very low values of the electric field allows us to explain our former numerical results [3], which had shown that some special Trojan wave packets are adiabatically connected with circular Rydberg states. It suggests that they can be generated from those states by adiabatic switching of a circularly polarized field. In Sec. V we present the energy spectra obtained numerically using an aligned states basis and we compare them to those obtained from the eigenvalues of Mathieu equation. Finally, in Sec. VI we discuss the results of a numerical experiment when the initial circular state is subjected to the action of the external circularly polarized field switched on quasiadiabatically. The paper concludes with a summary in Sec. VII.

II. TROJAN WAVE PACKETS AND QUANTUM PENDULUM

The quantum mechanical Hamiltonian of a hydrogen atom in a circularly polarized electromagnetic field written in the frame rotating with the field is given by (in a. u., $e=\hbar=m=1$)

$$H=\frac{\mathbf{p}^2}{2}-\frac{1}{r}+\mathscr{E}x-\omega L_z. \tag{1}$$

We assume that an eigenfunction of the Hamiltonian (1) with eigenvalue $E^j(\mathscr{E})$ can be expanded as

$$\Psi_E(r,\theta,\phi)=\sum_{n,l,m} c_{nlm}(E)R_{nl}(r)Y_{lm}(\theta,\phi), \tag{2}$$

where $R_{nl}(r)$ is the radial part of the hydrogenic eigenfunction and Y_{lm} is a spherical harmonic. In this basis the stationary Schrödinger equation with the Hamiltonian (1) takes the form

$$\mathscr{E}\sum_{n',l',m'} x_{nlm}^{n'l'm'} c_{n'l'm'}^{j} = [E^{j}(\mathscr{E}) - E_n + m\omega] c_{nlm}^{j}, \quad (3)$$

where j labels the exact (discrete) eigenvalues of (1), $E_n \equiv -1/2n^2$, and the hydrogenic dipole matrix elements $x_{nlm}^{n'l'm'}$ are known analytically [23].

Let us define $|nlm\rangle$ through the relation $\langle \mathbf{r}|nlm\rangle = R_{nl}(r)Y_{lm}(\theta,\phi)$ and divide the $\{|nlm\rangle\}$ basis we use into the manifolds $\{|n,n-1,n-1\rangle\}$, $\{|n,n-1,n-2\rangle\}\ldots$, $\{|n,n-k,n-k-s\rangle\},\ldots$. The first manifold represents circular states, the second all states with angular-momentum L_z one atomic unit lower, etc. For $k \ll n$ and $s \ll n$ (states with angular-momentum quantum numbers close to circular) matrix elements between states within a particular manifold labeled by k and s are much larger than those between states that belong to two different manifolds. This can be checked directly by inspecting the analytical form of the matrix elements of the coordinate x between two different hydrogenic eigenfunctions [23]. As a result, in a first approximation, the interaction between different manifolds can be neglected.

Additionally we concentrate on rotating-frame eigenfunctions that are well localized in angular-momentum space, namely, those requiring only a limited number of significant terms in the expansion (2) centered around some particular value of n denoted n_0. The dipole matrix elements between the states within a particular manifold are slowly varying functions of n and also slowly varying in k and s [23]. Because of the assumption of the localization of the wave function in angular momentum space we will put all matrix elements between states within a particular manifold equal. The conditions $k \ll n$ and $s \ll n$ allow us to take the value $x_{nlm}^{n'l'm'} = n_0^2/2 = r_0/2$ for all matrix elements assumed to be nonzero.

Under these assumptions Eq. (3) is block diagonal with blocks labeled by k and s. The assumption about the localization in n allows us to expand the hydrogenic energy around n_0 up to second order, namely,

$$E_n = -\frac{1}{2n_0^2} + \omega_c \delta n - \frac{3}{2}\frac{\delta n^2}{r_0^2}, \quad (4)$$

where $\omega_c = 1/n_0^3$ is the classical Kepler frequency corresponding to the quantum number n_0 and $\delta n = n - n_0$.

We assume the resonance condition $\omega_c = \omega$ and the Schrödinger equation (3) for a particular block then takes the simple form

$$\frac{\mathscr{E}}{2} r_0 (a_{n-1ks}^{j} + a_{n+1ks}^{j}) = \left[E^{j}(\mathscr{E}) - E_{n_0} + (n_0 - k - s)\omega + \frac{3}{2}\frac{\delta n^2}{r_0^2} \right] a_{nks}^{j}, \quad (5)$$

with $a_{nks} \equiv c_{n,n-k,n-k-s}$. This simplification follows directly from the fact that dipole matrix elements between states within a single manifold $\{|n,n-k,n-k-s\rangle\}$ are zero except between two consecutive states $|n,n-k,n-k-s\rangle$ and $|n-1,n-1-k,n-1-k-s\rangle$.

For n and l much larger than 1 we can assume that there is no boundary restriction for the variables n and δn. Under this assumption Eq. (5) is just the well known Mathieu equation written in Fourier space [24]. In real space it becomes

$$\left[\frac{3}{2}\frac{1}{r_0^2}\frac{\partial^2}{\partial\phi^2} + \mathscr{E} r_0 \cos\phi \right] f = [E^{j}(\mathscr{E}) - E_{n_0} + (n_0 - k - s)\omega] f. \quad (6)$$

Equation (6) is just Eq. (5) written in the $e^{i\delta n\phi}$ basis. It is also the Schrödinger equation for a quantum pendulum of mass $-\frac{1}{3}$ We can rewrite it in the standard Mathieu form [24]. Defining $\xi = (\phi - \pi)/2$ we get

$$\frac{\partial^2 f}{\partial \xi^2} + [\alpha - 2p\cos 2\xi] f = 0, \quad (7)$$

where

$$\alpha = -(8r_0^2/3)[E^{j} - E_{n_0} + (n_0 - k - s)\omega] \quad (8)$$

and the dimensionless parameter

$$p = \frac{4}{3}\frac{(e\mathscr{E}/m\omega^2)}{(\hbar^2/me^2)} = \frac{4}{3}\frac{\mathscr{E}}{\omega^2} \quad (9)$$

is proportional to the ratio between the radius of the orbit of a free electron in the presence of a circularly polarized light field (Volkov problem) and the Bohr radius (Coulomb problem).

Equation (7) has a discrete set of eigenvalues α_μ and two analytic asymptotic expressions are known [24]. For $p \ll \mu$ one gets

$$\alpha_\mu(p) \approx \mu^2 + \frac{p^2}{2(\mu^2 - 1)} \quad (10)$$

and in the opposite case for $\mu \ll p$ the asymptotic expression is

$$\alpha_\mu(p) \approx -\frac{(2\mu+1)^2 + 1}{8} + 2(2\mu+1)\sqrt{p} - 2p. \quad (11)$$

The corresponding eigenfunctions of Eq. (7) are Mathieu functions and because of periodic boundary conditions imposed on the wave function only those with periodicity π are permitted. This implies that in the case of formula (10) only every second eigenvalue can be permitted, namely, $\mu = 2j, j = 0,1\ldots$, since the eigenfunctions of (7) corresponding to odd μ have period 2π in the variable ξ and lead to nonphysical wave functions. In the case of formula (11), μ can be either even or odd since the solutions with periodicity π become approximately degenerate [24] with those with periodicity 2π and one corresponding to a physical solution can always be found.

The coefficients a_{nks}^{j} from Eq. (5) can be found as

$$a^j_{nks}=\int e_{2j}(\xi)e^{-2i\xi\delta n}d\xi, \tag{12}$$

where $e_{2j}(\xi)$ is the jth Mathieu function of period π. Expressions (10) and (11) allow us to obtain two asymptotic expressions for the field-dependent energy levels of the Hamiltonian. For low values of the electric field we obtain

$$E^j(\mathscr{E})\equiv E^j_{ks}(\mathscr{E})$$

$$=E_{n_0}-(n_0-k-s)\omega-\frac{3}{2}\frac{j^2}{r_0^2}-\frac{\mathscr{E}^2r_0^4}{4j^2-1}. \tag{13}$$

For larger field strengths we use (11) and get

$$E^j_{ks}(\mathscr{E})=E_{n_0}-(n_0-k-s)\omega$$

$$+\frac{3}{32}\frac{(2j^2+2j+1)}{r_0^2}-\left(j+\frac{1}{2}\right)\sqrt{\frac{3\mathscr{E}}{r_0}}+r_0\mathscr{E}. \tag{14}$$

The spectrum is labeled by three quantum numbers s, k, and j. The first two are associated with the angular-momentum quantum numbers of hydrogen and the third with excitations of the quantum pendulum. It is worth pointing out that the weak-field and the strong-field results of Eqs. (13) and (14) can be interpreted as the quadratic and approximately linear Stark effects in the frame rotating with the circularly polarized field.

The corresponding eigenfunctions can be written directly from (2)

$$\Psi_{jks}(r,\theta,\phi)=\sum_n a_{nks}R_{n,n-k}(r)Y_{n-k,n-k-s}(\theta,\phi). \tag{15}$$

Note that when the summation in (15) is restricted to n around some particular value n_0, as we assumed for the expansion of hydrogenic energy (4), the radial functions $R_{n,n-k}$ and $Y_{n-k,n-k-s}$ can be replaced by those for $n=n_0$. This is a result of the fact that for fixed s and k they have the same spatial character or, in other words, they are slowly varying functions of n. Under this assumption we get from (15)

$$\Psi_{jks}(r,\theta,\phi)=N_{n_0-k,n_0-k-s}e^{i(n_0-k-s)\phi}R_{n_0,n_0-k}(r)$$

$$\times P_{n_0-k,n_0-k-s}(\theta)\sum_{\delta n} a_{nks}e^{i\delta n\phi}, \tag{16}$$

where we have written the spherical harmonics Y_{lm} as products of the Legendre polynomial P_{lm}, the exponential $e^{il\phi}$, and the normalization factor N_{lm}. Note that now because of relation (12) the sum over δn can be reduced back to the Mathieu function and therefore the wave function has a nice analytical form

$$\Psi_{jks}(r,\theta,\phi)=N_{n_0-k,n_0-k-s}e^{i(n_0-k-s)\phi}R_{n_0,n_0-k}(r)$$

$$\times P_{n_0-k,n_0-k-s}(\theta)e_{2j}[(\phi-\pi)/2]. \tag{17}$$

We are particularly interested in the simplest eigenfunction ($j=0$, $k=1$, and $s=0$). In this case the functions R_{n_0,n_0-1}, P_{n_0-1,n_0-1}, and e_0 have Gaussian-like shapes in their coordinates [24,25]. Because of the connection with harmonic theory (explained later) we can identify this state with particular Trojan wave packets discussed previously [1,2]. For n_0 large enough and for appropriate field strengths the function (17) can be written as

$$\Psi_{jks}(r,\theta,\phi)=Ne^{i(n_0-1)\phi}e^{-(\omega/2)(r-r_0)^2}e^{-(\omega/2)r_0^2\theta^2}$$

$$\times e^{-\beta(\omega/2)r_0^2\phi^2}, \tag{18}$$

where the expression for the coefficient β is given by

$$\beta=\sqrt{\mathscr{E}_{sc}/3}. \tag{19}$$

Here $\mathscr{E}_{sc}$ is the electric field scaled to the Coulomb field at the distance r_0 from the nucleus $\mathscr{E}_{sc}=\mathscr{E}\omega^{-4/3}$.

The Gaussian approximation of the zeroth-order Mathieu function e_0 originates directly from the fact that the $\cos 2\xi$ in Eq. (7) can be replaced by its expansion up to second order in ξ when the wave function is compact enough to permit a small-ξ approximation. This occurs whenever p is large enough compared to μ. The Mathieu equation in this case becomes the Schrödinger equation of a harmonic oscillator. The quantum-mechanical condition for this replacement can be found from the requirement that if one wants the harmonic approximation to be valid for the jth eigenstate in Eq. (6) the amplitude of the cosine term in (6) must be larger than the energy of the jth level obtained from the harmonic approximation. This self-consistent requirement means that the cosine potential must be deep enough to bind j states in the harmonic portion of the potential well. This requirement gives the constraint for the scaled electric field, which is

$$\mathscr{E}_{sc}>3\frac{(j+1)^2}{n_0^2}. \tag{20}$$

This implies that for very small field strengths the harmonic approximation holds for the particular Trojan wave packets with $j=0$, and for j not far from the lowest the energy levels are almost equally spaced as predicted by formula (14). Note that wave function (18) only approximately satisfies periodic boundary conditions with respect to the variable ϕ and when it is well localized around $\phi=0$. On the other hand, the function (17) is free from this restriction since the Mathieu function e_0 has period π. In the limit $\mathscr{E}=0$ this function converges to the circular state whose Kepler frequency is the frequency of the circularly polarized light, which explains analytically our numerical results reported in [3].

III. RYDBERG MANIFOLDS AND HARMONIC OSCILLATORS

First we will revise and extend to the third dimension the harmonic analysis presented originally in [1] in Cartesian coordinates. The Hamiltonian (1) when written in cylindrical coordinates is

$$H=-\frac{1}{2}\left(\partial_r^2+\frac{1}{r}\partial_r+\frac{1}{r^2}\partial_\phi^2+\partial_z^2\right)-\frac{1}{\sqrt{r^2+z^2}}$$

$$+\mathscr{E}r\cos\phi+i\omega\partial_\phi. \tag{21}$$

After the transformation of the wave function $\Psi(r,\phi,z)=\Phi(r,\phi,z)/\sqrt{r}$ the Hamiltonian for the function Φ becomes

$$H=-\frac{1}{2}\left[\partial_r^2+\frac{1}{r^2}\left(\partial_\phi^2+\frac{1}{4}\right)+\partial_z^2\right]-\frac{1}{\sqrt{r^2+z^2}}$$

$$+\mathscr{E}r\cos\phi+i\omega\partial_\phi. \tag{22}$$

After dropping 1/4 in (22), performing the first unitary transformation $U_1=e^{il_0\phi}$, and then expanding the resulting Hamiltonian $H_1=U_1^\dagger H U_1$ up to second order in the operators ∂_r and ∂_ϕ and the variables $\delta r=(r-r_c)$, ϕ, and z [26] around the stable, circular, classical orbit [4], we obtain the quadratic Hamiltonian

$$H_1=E_0-\frac{1}{2}\left(\partial_r^2+\frac{1}{r_c^2}\partial_\phi^2+\partial_z^2\right)+\frac{\omega_r^2\delta r^2}{2}-\frac{\omega_\phi^2 r_c^2\phi^2}{2}$$

$$-2i\omega\frac{1}{r_c}\partial_\phi\delta r+\frac{\omega_z^2 z^2}{2}, \tag{23}$$

where the classical condition of the equilibrium of forces expressed by the equation

$$\omega^2 r_c+\mathscr{E}=\frac{1}{r_c^2} \tag{24}$$

implies vanishing of the linear terms and leads to the requirement $l_0=\omega r_c^2$. The frequencies ω_ϕ, ω_r, and ω_z are defined by the relations

$$\omega_\phi^2=\frac{\mathscr{E}}{r_c},$$

$$\omega_r^2=\omega^2+2\omega_\phi^2,$$

$$\omega_z^2=\omega^2-\omega_\phi^2 \tag{25}$$

and E_0 is the classical energy of the electron shifted by the rotation of the coordinate system

$$E_0=\frac{\omega^2 r_c^2}{2}-\frac{1}{r_c^2}+r_c\mathscr{E}-l_0\omega. \tag{26}$$

A second unitary transformation $U_2=e^{i\omega\delta r r_c\phi}$ next transforms the Hamiltonian (23) into

$$H_L=U_2^\dagger H U_2=E_0+\frac{\pi_r^2+\pi_\phi^2}{2}+\frac{-2q\omega^2X_r^2+q\omega^2X_\phi^2}{2}$$

$$-\omega(X_r\pi_\phi-X_\phi\pi_r)+\frac{\pi_z^2}{2}+\frac{\omega_z^2 z^2}{2}, \tag{27}$$

where we defined $X_r=\delta r$, $X_\phi=r_c\phi$, $\pi_r=-i\partial_r$, $(-i/r_c)\partial_\phi$, and $\pi_z=-i\partial_z$. The parameter q was defined in [1] as

$$q=\frac{1}{\omega^2 r_c^3} \tag{28}$$

and it can be interpreted as the ratio of the Coulomb force to the centrifugal force. It can be directly related to the scaled field $\mathscr{E}_{\rm sc}$ by the relation [1]

$$\mathscr{E}_{\rm sc}=(1-q)q^{-1/3}. \tag{29}$$

The part of the Hamiltonian (27) that is independent of z looks exactly like our harmonic Hamiltonian presented originally in [1]. The part dependent on z is decoupled from the rest of the Hamiltonian. This explains our claim that the essential physics of the problem can be obtained from an analysis in two dimensions. The Hamiltonian (27) can be written in diagonal form

$$H_L=E_0+\omega_+(a_+^\dagger a_++\tfrac{1}{2})-\omega_-(a_-^\dagger a_-+\tfrac{1}{2})$$

$$+\omega_0(a_0^\dagger a_0+\tfrac{1}{2}), \tag{30}$$

with the eigenfrequencies

$$\omega_+=\omega\sqrt{2-q+\sqrt{9q^2-8q}}\ \Big/\sqrt{2},$$

$$\omega_-=\omega\sqrt{2-q-\sqrt{9q^2-8q}}\ \Big/\sqrt{2},$$

$$\omega_0=\omega\sqrt{q}. \tag{31}$$

The operators a_+ and a_- can be expressed as complicated linear combinations of the operators X_r, π_r, X_ϕ, and π_ϕ, and a_0 has standard form. They are

$$a_+=\left(v\pi_r+i\frac{v}{M_\phi}\pi_\phi-\frac{i}{M_\phi}X_r-uX_\phi\right)\sqrt{N_+},$$

$$a_-=\left(-i\frac{v}{M_r}\pi_r-v\pi_\phi+uX_r+\frac{i}{M_r}X_\phi\right)\sqrt{N_-},$$

$$a_0=(i\pi_z+\omega_0 z)/\sqrt{\omega_0}, \tag{32}$$

with

$$N_+=2\frac{v}{M_\phi}(1-u),$$

$$N_-=2\frac{v}{M_r}(1-u),$$

$$M_r=\frac{1-2v\omega-v^2\omega_r^2}{u^2+2uv\omega+v^2\omega_\phi^2},$$

$$M_\phi=\frac{1-2v\omega-v^2\omega_\phi^2}{u^2+2uv\omega+v^2\omega_r^2}, \tag{33}$$

where u and v are the solutions of the system of equations

$$u-v\omega-uv\omega-v^2\omega_r^2=0,$$

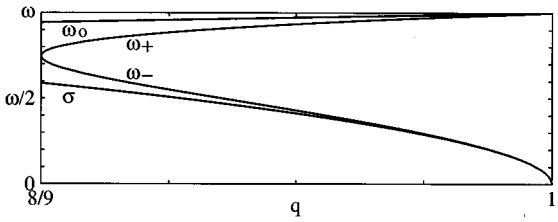

FIG. 1. Eigenfrequencies of the harmonic Hamiltonian (30) as functions of the parameter q and the spacing σ obtained from formula (36). Note that generally $\omega_0 \approx \omega_+ \approx \omega$ and $\sigma \approx \omega_-$, so the energy spectra obtained from the basis expansion method with the assumption about noninteracting manifolds and from the harmonic approximation approximately coincide. For lower field strengths (larger q) the agreement is better.

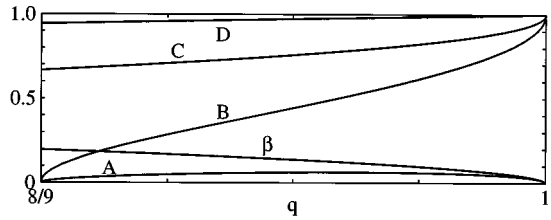

FIG. 2. Parameters of the Trojan wave packet obtained from the harmonic approximation in cylindrical coordinates as functions of the parameters q and β from the noninteracting manifolds model.

$$u + v\omega + uv\omega + v^2\omega_\phi^2 = 0. \tag{34}$$

Thus the spectrum of the Hamiltonian (21) within the three-dimensional harmonic approximation is

$$E_{m_+,m_-,m_0}(\mathscr{E}) = E_0 + (m_+ + \tfrac{1}{2})\omega_+ - (m_- + \tfrac{1}{2})\omega_- + (m_0 + \tfrac{1}{2})\omega_0. \tag{35}$$

The connection with the basis expansion method follows directly from formula (14). For the field strengths that guarantee classical stability [1] the parameter q satisfies the condition $(8/9) < q < 1$, so $q \approx 1$ and we have $\omega_+ \approx \omega$ and $\omega_0 \approx \omega$. For $\mathscr{E}$ large enough for fixed k and s, the energy levels given by expression (14) are equally spaced with the spacing

$$\sigma = \sqrt{(3\mathscr{E}/r_c)}. \tag{36}$$

The behavior of σ as a function of the parameter q (shown in Fig. 1) allows us to associate this spacing with the frequency ω_- from the harmonic approximation. Note additionally that $E_0 \approx E_{n_0} + \mathscr{E} r_c - (l_0 - 1)\omega$, since the radius of the classical orbit r_c is only a very little different from the radius of the corresponding Kepler orbit r_0. The small difference between those two radii is given by the relation $r_c = r_0/q^{1/3}$.

It is worth emphasizing that the magneticlike interaction term proportional to $\partial_\phi \delta r$, together with the quadratic potential hill in ϕ in the Hamiltonian (23), makes the effective electron mass fractional and negative $(-1/3)$, as expressed by the Schrödinger equation of an inverted pendulum (6). This results in the negative sign of the term with the frequency ω_- in the harmonic Hamiltonian (30).

IV. IDENTIFICATION OF TROJAN STATES

The connection between the basis expansion method and the harmonic approximation allows us to tell which Rydberg manifolds contribute most in creating the eigenfunctions of the Hamiltonian (30). The quantum number m_0 from the formula (35) associated with the excitation perpendicular to the plane of the motion of the packet obviously corresponds to the quantum number s in the expression (14). The quantum number m_+ in (35) corresponds to k in (14) and finally the Mathieu function index j corresponds to the index m_- in (35). Therefore the eigenstate of Hamiltonian (30) with the eigenvalue E_{m_+,m_-,m_0} is built mainly from the hydrogenic eigenfunctions that belong to the $\{|n, n-1-m_+, n-1-m_+-m_0\rangle\}$ manifold with n in the vicinity of n_0, which is defined by the resonance condition $\omega = 1/n_0^3$.

Let us consider a particular three-dimensional Trojan wave packet, the eigenfunction with the energy E_{000}. It contains in its expansion in terms of eigenfunctions of hydrogen mainly circular states with the principal quantum number n localized around n_0. For well-confined wave functions the factor $\sqrt{r}$ multiplying the function Φ can be replaced by $\sqrt{r_c}$ and the harmonic approximation in this case gives the following expression for the wave function Ψ (taking into account the action of the unitary transformations U_1 and U_2 as well):

$$\Psi(r,\phi,z) = N e^{i l_0 \phi} e^{-(\omega/2)[A(r_c\phi)^2 + B(r-r_c)^2]} \times e^{-(\omega/2)[2i(C-1)(r-r_c)r_c\phi + Dz^2]}. \tag{37}$$

The part of the wave function that depends only on ϕ and r can be obtained from our two-dimensional wave function in Cartesian coordinates [1] by a coordinate transformation up to second order [2]. The coefficients A, B, C were given in [1] as functions of q. The coefficient D characterizing the spread of the wave function around the plane of the circular motion can also be expressed in terms of the parameter q,

$$D = \sqrt{q}. \tag{38}$$

For large enough r_c and appropriate field strengths the wave function (37) can be compared directly with the expression (18) using the approximate relation $z = r_c\theta$. Note that when this approximation holds (for wave functions well localized around the plane of orbital motion) the circular coordinate r is approximately the same as the cylindrical r and a comparison is possible.

For lower field strengths when q is very close to 1 (Fig. 2) we have $B \approx C \approx D \approx 1$, and also $A \approx \beta$ (see Fig. 2), so those two wave functions do not differ too much from each other, which confirms the applicability of our model of noninteracting manifolds. The deviation for higher field strengths is a result both of the assumption of the lack of the interaction between manifolds as well as the fact that the basis of hydrogenic bound states is not a complete basis. The orthogonal space of the continuum states also exists, but the interaction with the continuum has been totally neglected. The interaction with the continuum states will lead to a small

amount of ionization, which we have observed numerically [2], and this contributes to a nonzero width of the energy levels.

Note that in the limit $l_0 \to \infty$ the harmonic approximation becomes exact [1] while the model of noninteracting manifolds does not and for very large l_0 the harmonic approximation should be used as a test of the former model rather than vice versa. For lower values of l_0 and lower field strengths, when the harmonic theory predicts weak radial confinement of the electron wave function, we can expect that the noninteracting manifolds model works better. In the limit $\mathscr{E} \to 0$ it recovers the quadratic nonlinearity of the Coulomb spectrum and the exact hydrogenic eigenfunctions. In particular the Trojan wave packet in this limit becomes a circular state and the limit can safely be taken because the wave function given in (15) is always periodic.

In the case of the function (37), the limit $\mathscr{E} \to 0$ can be taken only formally, since for very low electric-field values the harmonic approximation predicts large angular spreading of the wave function and the quadratic expansion is not well justified. Additionally, the function (37) strongly violates periodic boundary conditions for very low field strengths, when it is not well confined in coordinate ϕ.

V. NUMERICAL ANALYSIS

It is difficult to judge the range of validity of approximations based on inequalities such as $n \gg k$, etc. In this section we compare the energy spectra obtained by solving the stationary Schrödinger equation for Hamiltonian (1) using a reduced hydrogenic basis with the spectra obtained from Mathieu analysis. We show that our analytic approximations are remarkably well obeyed even for relatively low Rydberg quantum numbers. We also examine Trojan packet formation

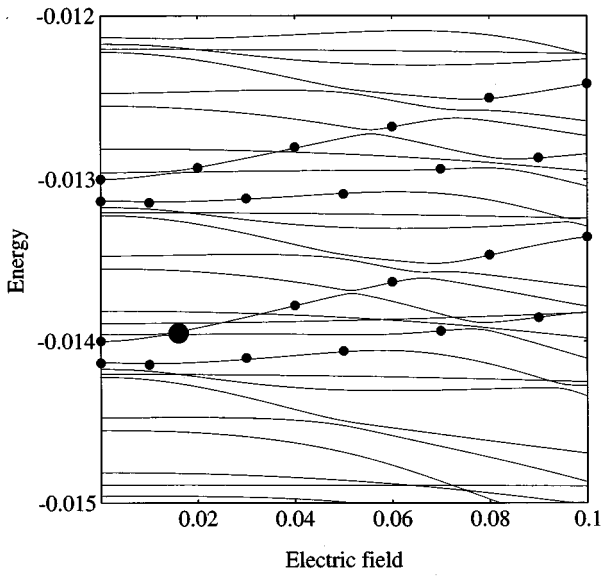

FIG. 3. Energy spectrum as a function of scaled electric field in the vicinity of the $n_0 = 10$ circular state for $\omega = 1/n_0^3$. The marker points belong to the Trojan lines. One can see two doublets on the diagram separated by approximately $\omega = 0.001$. The large marker point corresponds to the Gaussian-like Trojan packet for $\mathscr{E}_{sc} = 0.016$.

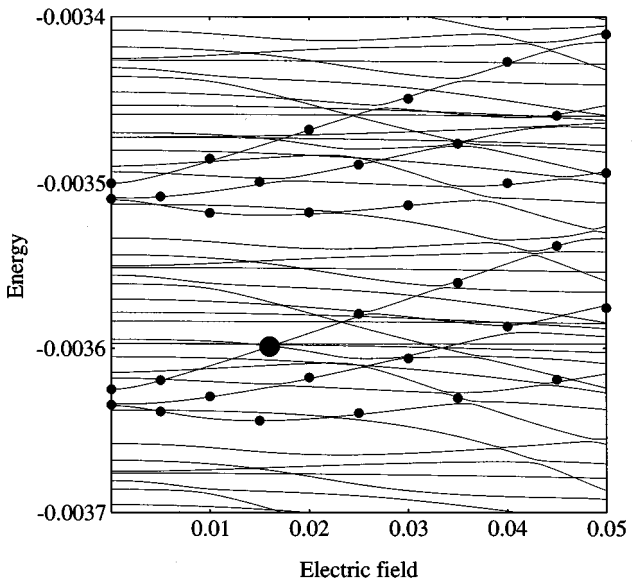

FIG. 4. Energy spectrum as a function of scaled electric field in the vicinity of the $n_0 = 20$ circular state for $\omega = 1/n_0^3$. The marker points belong to the Trojan lines. One can see two triplets on the diagram separated by approximately $\omega = 0.000\,125$. The large marker point corresponds to the Gaussian-like Trojan packet for $\mathscr{E}_{sc} = 0.016$.

by time-dependent numerical integration of the Schrödinger equation with the circularly polarized field switched on in a quasiadiabatic manner.

We have solved the stationary Schrödinger equation using only aligned states (states with $l = m$) in the expansion of the wave function (2), which is approximately equivalent to considering a two-dimensional hydrogen atom [27]. This corresponds to taking into account all (numerically truncated) states from $\{|n, n-1, n-1\rangle\}, \ldots, \{|n, n-k, n-k\rangle\}$ manifolds, with all interactions between those states governed by

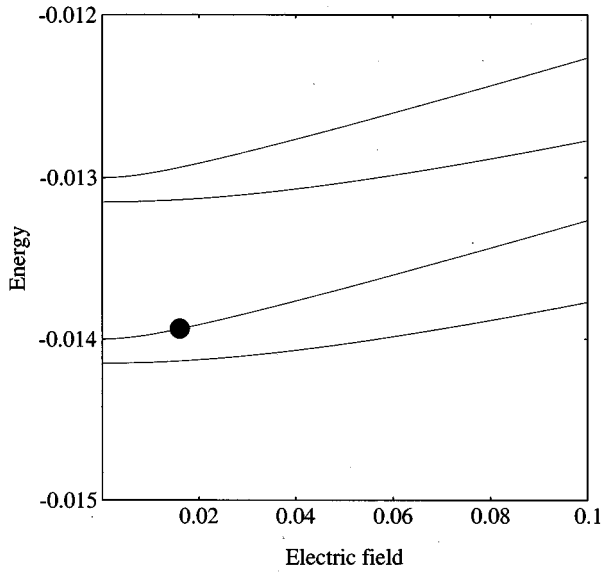

FIG. 5. Doublets obtained from the eigenvalues of Mathieu equation (7). As in Fig. 3, the large point corresponds to the Gaussian-like Trojan packet for $\mathscr{E}_{sc} = 0.016$.

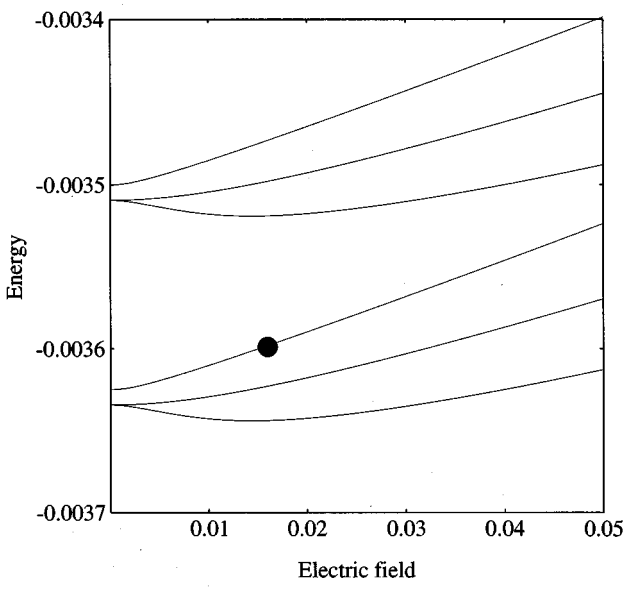

FIG. 6. Triplets obtained from the eigenvalues of Mathieu equation (7). As in Fig. 4, the large point corresponds to the Gaussian-like Trojan packet for $\mathscr{E}_{sc}=0.016$.

the values of the exact matrix elements between them.

Figures 3 and 4 show the rotating-frame energy spectra as functions of the scaled electric field for the frequency $\omega=1/n_0^3$, for $n_0=10$ and 20. One can barely identify two doublets in Fig. 3, but two triplets can be picked out in Fig. 4 consisting of energy lines almost linearly proportional to the field strength. This is the imprint of the harmonic spectrum. Note that from condition (20) one gets the maximum number of levels contributing to a harmoniclike structure within a single bunch as $n_{max}=n_0(\mathscr{E}_{sc}/3)^{1/2}$. For the maximum value of the scaled field $\mathscr{E}_{sc}=0.05$ and $n_0=20$ we get $n_{max}=2.58$, so one should expect about three harmonic energy lines as one sees in Fig. 4. For $\mathscr{E}_{sc}=0.1$ and $n_0=10$ we have $n_{max}=1.83$, so one expects to see up to two lines, as can be identified in Fig. 3. If the identification of the harmonic energies is not totally obvious, reference to Figs. 5 and 6, which show the corresponding energy lines obtained from the eigenvalues of Mathieu equation (7), is helpful. One can see very satisfactory agreement between analytical and numerical results for $n_0=20$ and still satisfactory for $n_0=10$.

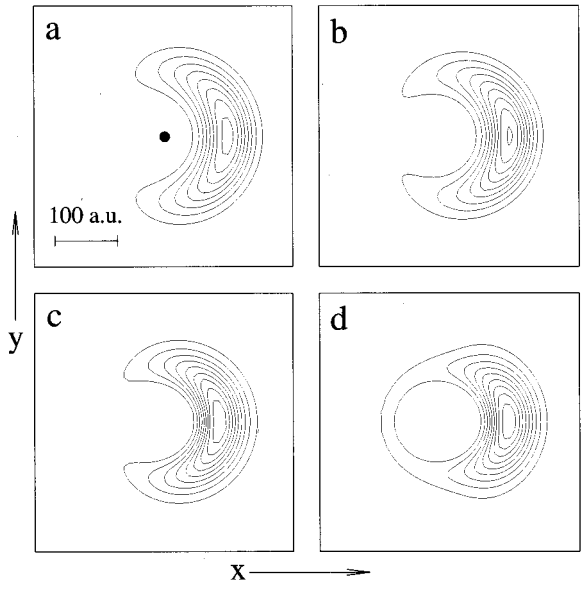

FIG. 7. Trojan wave packet for $\mathscr{E}_{sc}=0.016$ and $\omega=1/10^3$ obtained from (a) the harmonic approximation from formula (37), (b) the modified Gaussian approximation given by (40), (c) the Mathieu functions approach from expression (15), and (d) the solution in the aligned states basis (2). Functions (c) and (d) correspond to the two large points on the energy diagrams in Figs. 3 and 5. The gauge in the left lower corner of plot (a) indicates the distance equal to 100 a. u. The black dot in the center indicates the position of the nucleus ($x=y=0$).

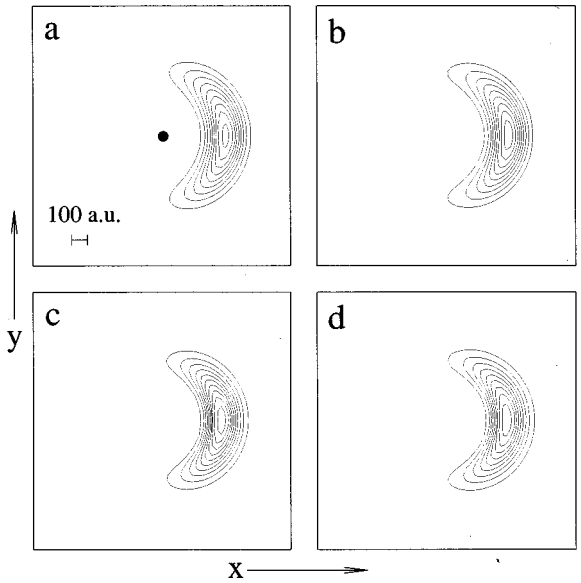

FIG. 8. Trojan wave packet for $\mathscr{E}_{sc}=0.016$ and $\omega=1/20^3$ obtained from various approximations as in Fig. 7. Functions (c) and (d) here correspond to the two large points on the energy diagrams in Figs. 4 and 6. The gauge in the left lower corner of plot (a) indicates the distance equal to 100 a. u. The black dot in the center indicates the position of the nucleus ($x=y=0$).

Our analysis formally confirms our former numerical result [3] that the wave functions that correspond to the eigenvalues from the energy line that ends at a particular circular state are Gaussian-like Trojan wave packets. The Kepler frequency of this circular state is in resonance with the frequency of the circularly polarized field. In Figs. 3 and 4 this is the line going through the large black point on the diagram.

Figures 7 and 8 show contour plots of two-dimensional versions of Trojan wave packet intensity (electron probability density) obtained from various approximations for the scaled field $\mathscr{E}_{sc}=0.016$ for $n_0=10$ and 20. Plots (a) show the result of the harmonic approximation discussed in Sec. III. In plots (b) we show Trojan packets obtained from the modified Gaussian approximation given by formula (40). Results of the Mathieu function approach and the aligned states expansion are shown in plots (c) and (d). In the case of functions given by the expansions (2) and (15), Legendre polynomials were replaced by a constant value and then the function was

normalized in two dimensions.

One can see that the difference increases when the value of n_0 decreases, but qualitatively all approaches give the same result. One expects the wave function obtained from the plain harmonic approximation to be the least accurate, since it significantly violates periodic boundary conditions for this value of the field.

VI. QUASIADIABATIC SWITCHING

The adiabatic connection between a Gaussian-like Trojan packet and its parent circular state implies [3] that a state originally prepared as a circular state will become angularly compact during the time evolution, if the electromagnetic field is switched on adiabatically. In this case the state will follow the Trojan energy line if one switches the field slowly enough not to cause transitions. This line has a series of crossings with other levels, some of them clearly avoided within the plot resolution (see Figs. 3 and 4), so the turn-on should also be diabatic enough to pass them and remain on the Trojan line. On this basis we predict Trojan packet formation to be feasible by an adiabatic switching that is conceptually extremely simple, depends on only the single parameter $\mathscr{E}$, and starts from a circular Rydberg state. Various techniques of circular state preparation have been reported [28–32].

In order to check this prediction we have solved the time-dependent Schrödinger equation numerically with the two-dimensional version of the circular state $n_0=20$ taken for the initial condition. The frequency of the circularly polarized field was tuned to the Kepler frequency of this state $\omega=1/n_0^3$. The field was switched on exponentially during twenty optical cycles according to the formula $\mathscr{E}(t)=\mathscr{E}_0 e^{-0.2(t-20)}$ until the value $\mathscr{E}_0=0.016\omega^{-4/3}$ was reached ($\mathscr{E}_{sc}=0.016$). After the turn-on was complete we monitored an additional ten cycles of evolution with the constant value of the amplitude $\mathscr{E}=\mathscr{E}_0$. Figure 9 confirms our prediction. It shows the formation of a sharply angularly localized packet during the adiabatic switching process.

To check this confirmation quantitatively, we have also calculated the testing functions

$$C(t)=\left|\int \Phi^*\Psi d\mathbf{r}\right|^2,$$

$$R(t)=\int_{\mathscr{R}}|\Phi|^2 d\mathbf{r},$$

$$P(t)=\int |\Phi|^2 d\mathbf{r}. \tag{39}$$

Here the wave function Φ is a numerical solution of the full time-dependent Schrödinger equation, such as that shown in Fig. 9, and the wave function Ψ is obtained from our modified Gaussian approximation [2] with $\mathscr{E}$ chosen to be the final field strength $\mathscr{E}_0$ reached during the switching. That is, Ψ is given in two dimensions by

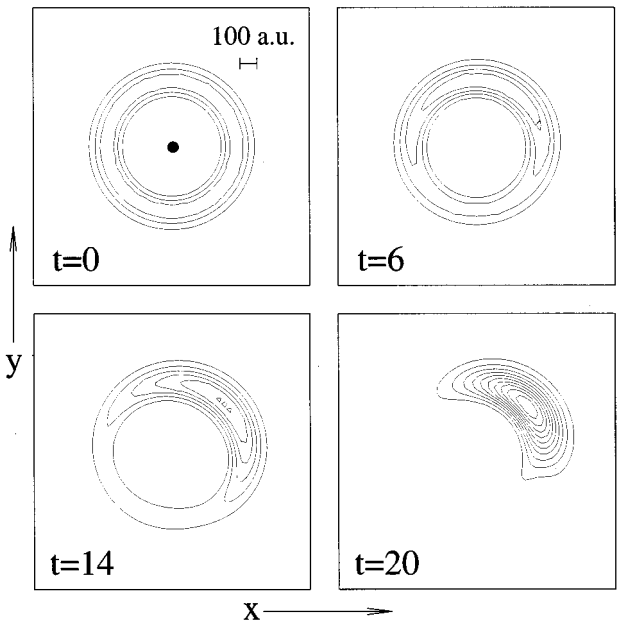

FIG. 9. Adiabatic angular localization of electron probability density. Snapshots of $|\Phi|^2$ at $t=0$ and after 6, 14, and 20 cycles show increasing angular bunching during exponential switching of the field. The initial state is the circular state for $n_0=20$. The gauge in the right upper corner of plot (a) indicates the distance equal to 100 a. u. The black dot in the center indicates the position of the nucleus ($x=y=0$).

$$\begin{aligned}\Psi(r,\phi)&=Ne^{il\phi}\exp\{-(l/2r_c^2)[2r_c^2 a(1-\cos\phi)\\&\quad+b(r-r_c)^2+2icr_c(r-r_c)\sin\phi]\}\\&=Ne^{il\phi}\exp\{-(l/2r_c^2)[4r_c^2 a\sin^2(\phi/2)\\&\quad+b(r-r_c)^2+4icr_c(r-r_c)\sin(\phi/2)\\&\quad\times\sqrt{1-\sin^2(\phi/2)}]\},\end{aligned} \tag{40}$$

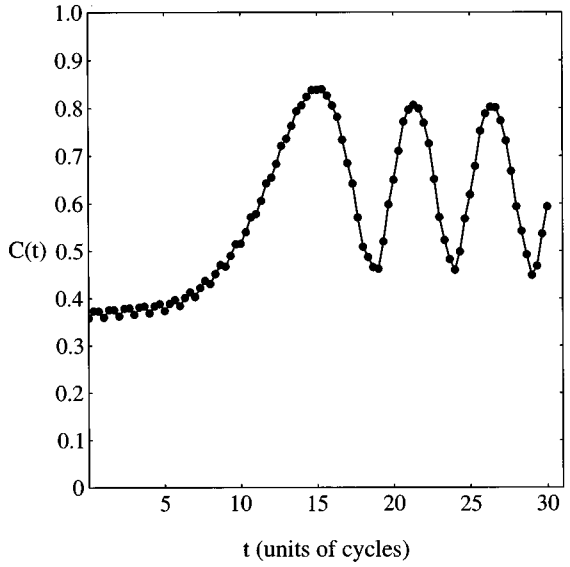

FIG. 10. Correlation function $C(t)$ as defined in (39).

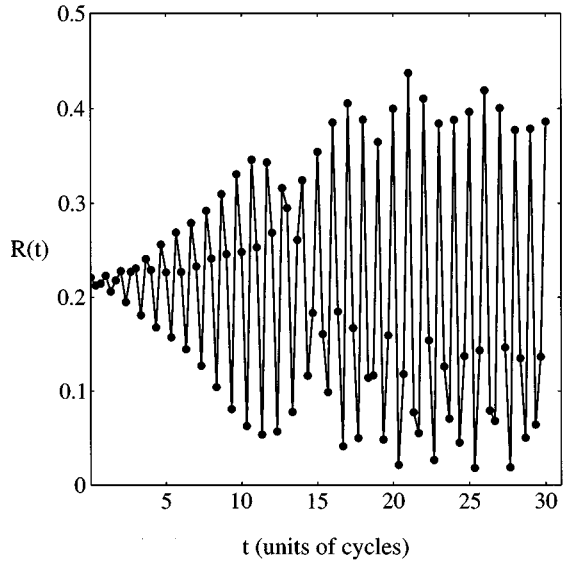

FIG. 11. Localization function $R(t)$ as defined in (39). The amplitude of this function grows as probability localizes since the packet periodically sweeps a fixed rectangle.

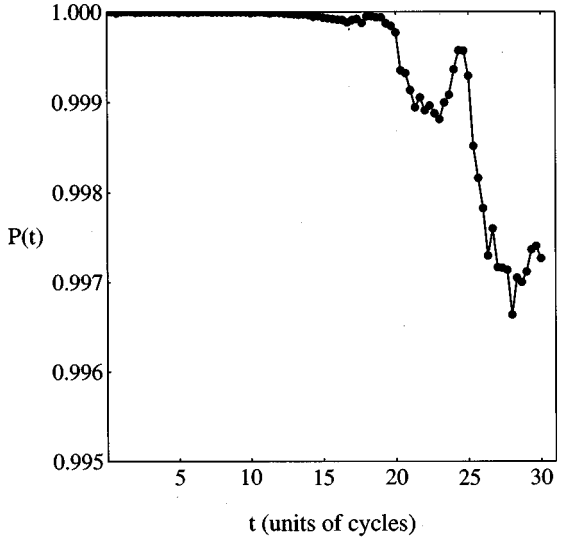

FIG. 12. Total electron probability $P(t)$ as defined in (39). The values along the P axis emphasize the negligible loss to ionization.

with the parameters

$$l=20,$$

$$r_c=388.69,$$

$$a=0.057\,06, \quad b=0.716\,56, \quad c=-0.138\,60. \quad (41)$$

The letter $\mathscr{R}$ refers to a specific area of integration. $\mathscr{R}$ is defined as the rectangle in the laboratory frame that contains 60% of the probability calculated from the initial wave function (40): $\int_{\mathscr{R}}|\Psi|^2 d\mathbf{r}=0.6$ at $t=0$.

The growth of the correlation function C plotted in Fig. 10 shows that a state with a large component of Trojan packet is actually generated. The amplitude increase of the function R, as shown in Fig. 11, is also evidence of localization. The quantity $P(t)$ is the total probability in a circle concentric with the packet orbit, with radius $2r_c$. It is important to note that the probability of escape out of the circle is negligible. This is represented by the decrease of the function P, which is shown in Fig. 12, and is a useful measure of ionization.

VII. SUMMARY AND CONCLUSIONS

In conclusion, we have shown how the presence of the external field can suppress the nonlinearity of the Coulomb spectrum and can produce a harmonic spectrum. This spectrum agrees with the one found by an explicit harmonic approximation [1]. Our model of noninteracting Coulomb manifolds explains why the harmonic structure appears in the energy levels even for low angular momenta, when the harmonic approximation originally introduced in [1] may not be well justified. This approach is especially useful for those who would like to observe Trojan wave packets numerically for lower values of the circularly polarized fields by integrating Schrödinger's equation using a hydrogenic basis expansion rather than a spatial grid integration [2], since it tells which states from the eigenspace of hydrogen should be used in the expansion of the time-dependent wave function. It also permits a strong prediction that Gaussian-like Trojan wave packets are adiabatically connected with circular Rydberg states whose Kepler frequency matches the frequency of the circularly polarized light. The numerical experiment presented here fully confirms those predictions.

ACKNOWLEDGMENTS

We acknowledge with pleasure frequent discussions with I. Bialynicki-Birula. This research was supported by the National Science Foundation under Grants Nos. INT93-11766 and PHY94-08733

[1] I. Bialynicki-Birula, M. Kalinski, and J. H. Eberly, Phys. Rev. Lett. **73**, 1777 (1994).
[2] M. Kalinski, J. H. Eberly, and I. Bialynicki-Birula, Phys. Rev. A **52**, 2460 (1995).
[3] M. Kalinski and J. H. Eberly, in *Coherence and Quantum Optics VI*, edited by J. H. Eberly, L. Mandel, and E. Wolf (Plenum, New York, in press).
[4] H. Klar, Z. Phys. D **11**, 45 (1989).
[5] D. Farrelly and T. Uzer, Phys. Rev. Lett. **74**, 1720 (1995).
[6] E. Madelung, Z. Phys. **40**, 322 (1926); see also I. Bialynicki-

Birula, M. Cieplak, and J. Kaminski, *Theory of Quanta* (Oxford University Press, New York, 1992), p. 88.
[7] I. Bialynicki-Birula, M. Kalinski, and J. H. Eberly, Phys. Rev. Lett. **75**, 973 (1995).
[8] A. Buchleitner and D. Delande, Phys. Rev. Lett. **75**, 1487 (1995).
[9] J. E. Bayfield and P. M. Koch, Phys. Rev. Lett. **33**, 258 (1974).
[10] P. Fu, T. J. Scholz, J. M. Hettema, and T. F. Gallagher, Phys. Rev. Lett. **64**, 511 (1990).
[11] J. E. Bayfield, Chaos **1**, 110 (1991).
[12] L. D. Noordam, H. Stapelfeldt, D. I. Duncan, and T. F. Gallagher, Phys. Rev. Lett. **68**, 1496 (1992).
[13] P. M. Koch, Chaos **2**, 131 (1992).
[14] B. E. Sauer, M. R. W. Bellermann, and P. M. Koch, Phys. Rev. Lett. **68**, 1633 (1992).
[15] M. Gatzke, B. Broers, L. D. Noordam, R. B. Watkins, and T. F. Gallagher, Phys. Rev. A **50**, 2502 (1994).
[16] L. Sirko, M. Arndt, P. M. Koch, and H. Walther, Phys. Rev. A **49**, 3831 (1994).
[17] G. M. Lankhuijzen and L. D. Noordam, Phys. Rev. Lett. **74**, 355 (1995).
[18] J. A. Yeazell and C. R. Stroud, Jr., Phys. Rev. Lett. **60**, 1494 (1988).
[19] A. ten Wolde and L. D. Noordam, Phys. Rev. A **40**, 485 (1989).
[20] J. A. Yeazell, M. Mallalieu, and C. R. Stroud, Jr., Phys. Rev. Lett. **64**, 2007 (1990).
[21] J. A. Yeazell, G. Raithel, L. Marmet, H. Held, and H. Walther, Phys. Rev. Lett. **70**, 2884 (1993).
[22] M. W. Noel and C. R. Stroud, Jr., Phys. Rev. Lett. **75**, 1252 (1995).
[23] H. A. Bethe and E. E. Salpeter, *Quantum Mechanics of One and Two-Electron Atoms* (Springer-Verlag, Berlin, 1957).
[24] N. W. McLachlan, *Theory and Application of Mathieu Functions* (Oxford University Press, New York, 1947).
[25] L. S. Brown, Am. J. Phys. **41**, 525 (1973).
[26] This procedure is slightly different from the quadratic approximation in real space of the variables r and $\sin(\phi/2)$ used in [2] and is equivalent to dropping some small terms of order $1/l_0$ [2]. Keeping those terms leads to more accurate wave functions but it also leads to a nonlinear system of equations that can no longer be handled analytically [2]. Note, for example, that the term $\delta r \partial_\phi^2$ is dropped here as third order even if it can generate second-order terms in the real-space variables δr and ϕ when acting on the wave function.
[27] X. L. Yang, S. H. Guo, and F. T. Chan, Phys. Rev. A **43**, 1186 (1991).
[28] R. G. Hulet and D. Kleppner, Phys. Rev. Lett. **51**, 1430 (1983).
[29] J. Hare, M. Gross, and P. Goy, Phys. Rev. Lett. **61**, 1938 (1988).
[30] P. Nussenzveig, F. Bernardot, M. Brune, J. Hare, J. M. Raimond, S. Haroche, and W. Gawlik, Phys. Rev. A **48**, 3991 (1993).
[31] R. J. Brecha, G. Raithel, C. Wagner, and H. Walther, Opt. Commun. **102**, 257 (1993).
[32] C. H. Cheng, C. Y. Lee, and T. F. Gallagher, Phys. Rev. Lett. **73**, 3078 (1994).